Technetium-99m-d,l-Hexamethylpropyleneamine Oxime (HMPAO) Uptake and Glutathione Content in Brain Tumors

E. Suess, S. Malessa, K. Ungersböck, P. Kitz, I. Podreka, K. Heimberger, O. Hornykiewicz, and L. Deecke

Clinic of Neurology, Department of Biochemical Pharmacology, and Clinic of Neurosurgery, University of Vienna, Vienna, Austria

Technetium-d,HMPAO SPECT was performed in 70 patients suffering from intracerebral tumors of various histologic types (glioma n = 30, meningeoma n = 19, metastases n = 10, angioma n = 3, neuroma n = 2, lymphoma n = 2, neurocytoma n = 1, epidermoid n = 1, gliosis n = 1, cholesteatoma n = 1). Tumor classification was histologically verified in all subjects except in two cases with inoperable angiomas. SPECT was performed under resting state conditions with a dual-head rotating camera (SIEMENS ZLC 37) following intravenous injection of 18–25 mCi ^{99m}Tc-d,l-HMPAO. Regional tracer deposit was expressed in terms of a cerebellar index (CBI). Significantly higher regional HMPAO uptake was found in meningeomas when compared with gliomas of different malignancy (ANOVA $p < 0.05$). Within gliomas, regional uptake increased with malignancy (n.s.). In 23 patients, a total of 32 tumor specimens were obtained for histochemical analysis of glutathione (GSH) content using high-pressure liquid chromatography. A significant correlation (least square method, $p < 0.001$) between CBIs and GSH values was found, supporting the hypothesis that GSH is the predominant factor for the conversion of the lipophilic complex to hydrophilic derivates.

J Nucl Med 1991; 32:1675–1681

Since ^{99m}Tc-d,l-hexamethylpropyleneamine oxime (^{99m}Tc-d,l-HMPAO, Ceretec®, Amersham Intl.) was first introduced as a tracer for rCBF imaging (*1–3*), its use in various states of diseases has been extensively evaluated (*4*). The potential value of HMPAO as a tumor blood flow agent was first demonstrated in non-cerebral animal tumors (*5*). In human brain tumors, controversial observations were reported on the uptake behavior of this ligand (*6*). Lindegaard et al. (*7*) reported low regional uptake in 10 of 12 patients with gliomas. In contrast, Babich et al. (*8*) described a greater variation of areas with markedly increased tracer deposit as well as photopenic ones. A close relation of d,l-HMPAO distribution in gliomas compared to tumor blood flow measured with $C^{15}O_2$ and PET was reported from Langen et al. (*9*).

d,l-HMPAO is a lipophilic technetium complex that freely crosses the intact blood-brain barrier. Following initial washout, it remains trapped in the brain without relevant redistribution over a period sufficient for data acquisition using a gamma camera. In vitro studies have shown that the d,l-HMPAO decomposition rate linearly depends on present glutathione (GSH) concentrations (*10*). Glutathione represents the major amount of free thiols in mammalian tissues and protects cells from oxidative challenge. It was concluded that GSH is the predominant factor for conversion from the lipophilic form to hydrophilic derivatives. The measurement of regional GSH concentration in the human brain, however, is critical due to rapid enzymatic conversion of GSH in postmortem studies (*11*) and consistent data about normal GSH levels in different brain regions are not available at present. Since most of the patients suffering from brain tumors undergo surgical tumor resection, this therapeutic approach offers easy access to tumor specimens for GSH determination.

In the controversial discussion about CBF quantification with d,l-HMPAO SPECT, the intracellular retention mechanism still plays a crucial role. If the assumptions hold true that the retention of d,l-HMPAO is predominantly GSH-dependent and that the conversion rate is uniform in all brain tissues, one would expect a statistically significant correlation between tissue GSH concentrations and regional tracer uptake in SPECT studies. The purpose of the present study is to test this hypothesis.

MATERIALS AND METHODS

Patients

A total of 70 patients (male n = 33; female n = 37) with intracerebral tumors (glioma n = 30 (mean age = 50.17 ± 15.28; male 13, female 17), meningioma n = 19 (mean age = 62.9 ± 13.5; male 8, female 11), angioma n = 3 (mean age = 35.3 ± 22.3, male 2, female 1), metastases n = 10 (mean age = 54.7 ± 15.3, male 5, female 5), neuroma n = 2, lymphoma n = 2, neurocytoma = 1, epidermoid n = 1, gliosis n = 1, cholesteatoma n = 1) was investigated using d,l-HMPAO-SPECT. In all subjects,

Received Aug. 3, 1990; revision accepted Jan. 29, 1991.
For reprints contact: Erhard Suess, MD, Clinic of Neurology, University of Vienna, Lazarettgasse 14, A-1090 Vienna, Austria.

the diagnostic procedure included clinical investigation, CAT, and four-vessel intra-arterial angiography. All CAT investigations were performed with and without contrast enhancement in the same session. Both CAT and SPECT were carried out within 2 to 4 days. SPECT was performed prior to surgery and prior to radiation or chemotherapy respectively in all but four patients with tumor regrowth at least 6 mo after craniotomy. Tumor classification was histologically verified, based on open-tumor resection, according to current WHO criteria. In two cases with inoperable angiomas, the diagnoses were made neuroradiologically.

d,HMPAO SPECT Studies

SPECT was performed with a dual-head rotating scintillation camera (Siemens Dual Rota ZLC 37) equipped with parallel-hole HIRES collimators (FWHM 12 mm). Sodium perchlorate (500 mg) was given before tracer administration. Eighteen to 25 mCi (666–925 MBq) of d,l-HMPAO were injected intravenously immediately after formulation of the kit, following the instructions of the producer. A detailed description of data acquisition and image reconstruction procedures used in our laboratory was given earlier (*4*). For final evaluation, seven single slices (3.125 mm thick) were summed consecutively to obtain a set of 21.9-mm thick transverse sections covering the whole brain. The reproducibility of our SPECT system was evaluated earlier in a quantitative phantom study (*12*). For volumes of 14.5 ml, highly reproducible values were obtained. Considering the recommendations of Mazziotta et al. (*13*), the in-plane resolution limit of reconstructed SPECT tomogram was twice the FWHM of 12 mm (HIRES collimators).

For data evaluation two regions of interest (ROIs) were drawn in two representative summed cross sections: one around the tumor margin as indicated by CAT images and the other circumscribing the ipsilateral cerebellum. To avoid interobserver variabilities, all ROIs were drawn by a single, anatomically trained neurologist (E.S.). Planar slices of contrast-enhanced CAT and SPECT tomograms, representing about the same orbitomeatal line, were compared together visually by an experienced neuroradiologist (K.H.). For semiquantification of tumor uptake, a tumor-to-cerebellum ratio [cerebellar index; CBI = average cts per pixel (tumor ROI)/average cts per pixel (cerebellar ROI)] was calculated, indicating relatively high and low tracer uptake referring to the cerebellum. This procedure is identical with that described by Langen et al. (*14*). The ipsilateral cerebellum was chosen to avoid errors due to cross-cerebellar diaschisis (CCD) as described previously (*7*). In normals, an interhemispheric difference of regional HMPAO retention exceeding 12% was considered as pathologic (*4*). Likewise, a significant interhemispheric asymmetry in the cerebellum was estimated by a color-coded display, with colors separated by 12% steps. Thus, CCD was diagnosed in patients with frontal lesions, when the cerebellar asymmetry exceeded 12% (n = 21).

In those cases in which GSH concentration was measured, additional ROIs were drawn representing the location from which tumor specimens were taken. The placement of these ROIs was guided by the description of the surgeon (cortex, tumor border, tumor center, approximate distance from craniotomy). To avoid errors due to the partial volume effect, ROIs exceeded the size of tissue specimens (matrix size of ROIs greater than 8 × 8 pixels; pixel size: 9,765 mm^2).

Determination of GSH Content

In 23 patients, a total of 32 biopsy specimens (glioma n = 15; meningioma n = 10; metastasis n = 5; neurocytoma n = 1; neurinoma n = 1) were obtained for quantitative GSH determination using high-pressure liquid chromatography (HPLC).

Brain tumor specimens were obtained during craniotomy, immediately dropped into liquid nitrogen, and kept frozen at −196°C. After weighing the tissue, samples were homogenized in 10 vol of ice-cold 0.4 *M* perchloric acid and centrifuged. Supernatants were stored at −70°C for 2 days to 6 wk and thawed just before analysis. Twenty-five microliters of supernatant—equivalent to 2.5 mg fresh tissue—were analyzed. For separation of amino acids, a 3.1-mm × 25-cm column, packed with BioRad Aminex HP-C cation exchange resin and a step gradient of buffers (0.2 *M* Natrium-formiat adjusted to a pH of 2.75 with phosphoric acid followed by 0.2 *M* Natrium-acetic acid, pH 5.55) was used. This procedure allowed a clear separation of GSH from aspartic acid. The eluate was mixed continuously with 0.5 *M* borate buffer, pH 11.2, containing 0.1% mercaptoethanol and 1% ophthaldialdehyde. The fluorescent derivatives were measured by an Amino fluorometer equipped with a 70-μl quartz flow cell, a Corning 7–51 primary filter, and a Wratten 8 secondary filter. Fluorescence was detected at 360 nm excitation and 450 nm emission wavelength. Chromatograms were integrated automatically and compared to external standards containing GSH (1.5 g/l) as well as various amino acids (modified after reference 15). This method revealed quantitative GSH content in tissue probes (nmol/mg wet weight).

MAb Factor VIII Immunostaining

To reveal information about the vascular compartment in tumors, a morphometric measurement of tumor specimens by means of a ratio between the total amount of vascular area and the determined tumor area was performed using the MAb Factor VIII immunostaining technique. Eleven samples were evaluated in nine patients (meningioma n = 5, glioma n = 4, metastasis n = 2).

Adequate portions of tumor tissue sampled for the GSH determination were fixed in buffered formalin and embedded in paraffin. Paraffin sections were stained immunohistologically with the MAb Factor VIII (DAKO) using the indirect ABC technique. Counterstain was done with Hämalaun. In the light microscope, all tissue sections were evaluated planimetrically by a modified point counting method described elsewhere (*16*). One to 2 cm^2 of each tumor tissue, i.e., six to eight visual fields at low magnification range, were investigated. Thus, the total amount of vascular area, defined by MAb Factor VIII stained endothelial layer, was determinated quantitatively. The ratio between the tumor area and the vascular area was calculated and expressed as a percentage. A higher percentage was generally found in tumors with increased vascular density of sinusoidal vessels. In contrast, tumor biopsies composed of larger areas without a higher number of venules were represented by lower percentual values. Thus, highly vascularized tumors were assumed to contain more blood volume than those with low vascular density.

RESULTS

Comparison of HMPAO Uptake in Different Brain Tumors

When SPECT images were estimated visually, regional tracer deposit appeared to be abnormal in all cases. The

location and the extention of regional abnormalities agreed well with tumor delineation seen in CAT images. In those cases, however, where low uptake and perifocal edema dominated, visual discrimination of tumor borders was partially limited in SPECT tomograms and contrast-enhanced CAT had to be used as a reference (n = 12). Due to blood-brain barrier permeability alterations, CAT showed low contrast enhancement in many cases in the edema as well. In this study, however, the contrast was sufficient for clear discrimination of tumor margins in all instancies when CAT was used as a reference. When a tumor-to-cerebellum ratio of 1% ± 5% (range of CBI: 0.95–1.05) was assumed as normal range, cerebellar indices were within these limits in six patients (meningiomas 3, metastases 2, lymphoma 1). In low-grade astrocytomas (I–II), regional tracer uptake was lower than in the cerebellum in all except one case (CBI = 1.067). In Grade III astrocytomas both relatively high as well as relatively low uptake was observed. These tumors could be discriminated from lower grade astrocytomas due to higher regional uptake or to perifocal edema. Grade IV glioblastomas were identified by inhomogenous uptake within tumor borders as well as perifocal edema. Typically, a low uptake zone in the tumor center was found, representing central necrosis surrounded by a high uptake zone. Alterations of normal brain structures due to mass effects and infiltrating tumor growth were frequently observed in Grades III and IV gliomas (Fig. 1).

In meningiomas, a high and rather homogenous tracer deposit was seen predominantly. These tumors were typically located close to meningeal structures. In three cases, CBIs were within the range of cerebellar values. Since the cerebellum generally shows the highest tracer uptake in the brain, these tumors appeared as high uptake zones compared to non affected brain tissue. Likewise, in only two patients with calcified meningeomas was low regional uptake observed (Fig. 2). A controversial observation was made in angiomas, where one of three studies revealed high tracer uptake in the tumor region (CBI = 1.25) (Fig. 3).

Uptake behavior in metastases varied. Tracer deposit appeared to be low in those patients in whom bronchogenic (n = 3), breast (n = 2), chondrosarcoma (n = 1), or melanoma (n = 1) were the primary neoplasms. High uptake was seen in patients with hypernephroma (n = 2) and in a highly malignant epithelial metastasis of unknown origin (Fig. 4).

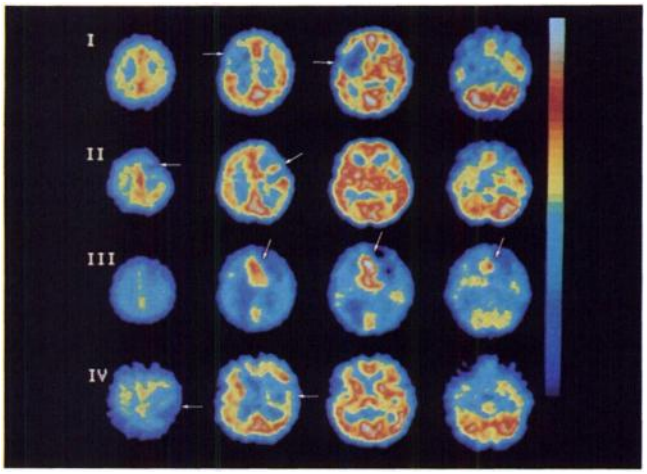

FIGURE 1. Gliomas. (Case I) Transverse cross sections (cranial = left; caudal = right, frontal = top) in a 21-yr-old female with rightsided hemiparesis. SPECT shows low uptake in the left meso and inferior frontal lobe indicating astrocytoma I. CBI = 0.598. (Case II) Transverse cross sections in a 38-yr-old female with minimal hemiparesis of the left side. SPECT shows low uptake in the right superior and mesofrontal region and in the right insula indicating astrocytoma II. Notice that the right central region is partially unaffected (see second slice). CBI = 0.69. (Case III) Transverse cross sections in a 21-yr-old female with clinical findings according to intracranial pressure syndrome. SPECT shows high tracer uptake in the great commissure and uptake deficit in the right superior frontal region, indicating astrocytoma III. CBI = 1.324, GSH = 1.58 nmol/mg. (Case IV) Transverse cross sections in a 78-yr-old female. According to the stroke-like occurrence of left-sided hemiparesis a progressive stroke was initially diagnosed. SPECT shows circular tracer uptake atypically located in the right hemisphere (second slice) surrounding a low uptake area (necrosis), indicating glioblastoma IV. CBI = 0.65, GSH = 0.77 nmol/mg.

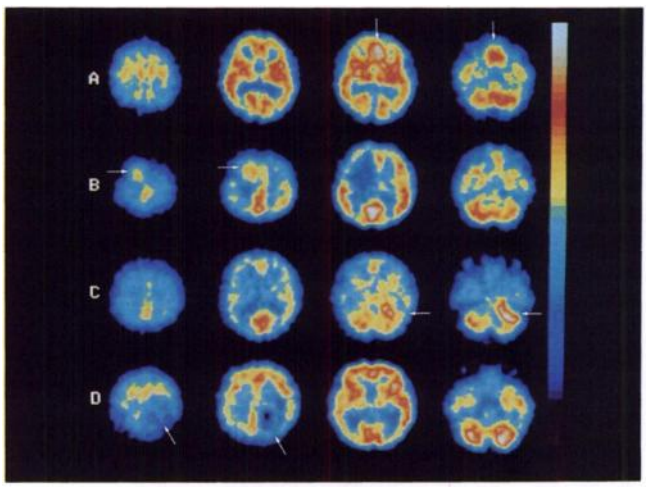

FIGURE 2. Meningiomas. (A) Transverse cross sections in a 80-yr-old male with a meningioma originating from falx cerebri. The predominant symptoms were a psychoorganic syndrome associated with hallucinatory events. SPECT shows high tracer uptake in the fronto-basal midline (third slice). CCD is seen in the left cerebellum. CBI = 1.065. (B) Transverse cross sections in a 57-yr-old female with clinically evident right-sided hemiparesis. SPECT shows a high uptake area in the left frontopolar region surrounded from a low uptake zone (edema) in the ipsilateral hemisphere. CCD is seen in the contralateral cerebellum. CBI = 1.265, GSH = 4.37 nmol/mg. (C) Transverse cross sections in a 45-yr-old female with cerebellopontine angle syndrome. SPECT shows high uptake in the right cerebellopontine angle. CBI = 1.308. (D) Transverse cross sections in a 71-yr-old female with homonymous hemianopia of the left visual hemifield. SPECT shows uptake deficiency in the right occipital region, indicating a calcified meningioma. CBI = 0.328, GSH = n.d.

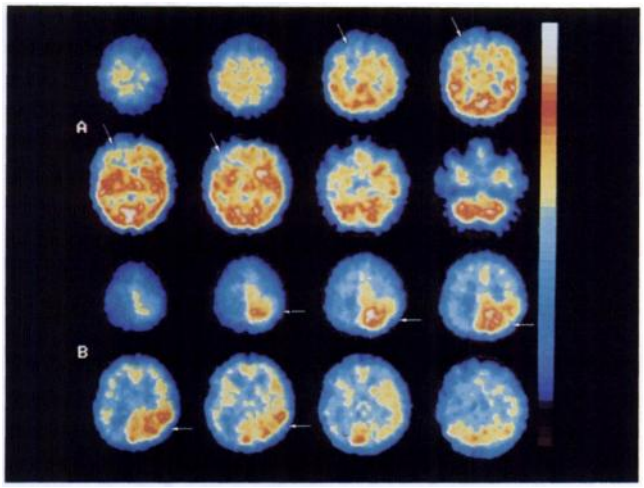

FIGURE 3. Angiomas. (A) Eight transverse cross sections (first and second row) in a 61-yr-old female with angioma verified by angiography. SPECT shows low uptake in the left frontal lobe. CBI = 0.71. (B) Eight transverse cross sections (third and fourth row) in a 21-yr-old female with a vascular malformation in the right occipito-parietal region. SPECT shows high but inhomogenous tracer deposit in the affected location. CBI = 1.25.

Furthermore, high uptake was found in neurocytoma (n = 1) and one lymphoma, and low uptake was found in one epidermoidal tumor. In gliosis (n = 1) and in another lymphoma, tracer uptake appeared to be higher than the surrounding, nonaffected brain tissue, although CBIs were close to 1. In acoustic neuroma (n = 2), HMPAO uptake appeared similar to normal cortical brain tissue. These tumors, however, were located typically in the cerebellopontine angle and were therefore easily recognized.

Cross-cerebellar diaschisis was observed in patients with frontal lesions and low tracer deposit in the contralateral cerebellum, when the cerebellar asymmetry exceeded 12% (see Material and Methods). These criteria were fulfilled in 21 patients (gliomas n = 12, meningiomas n = 5, metastases n = 2, lymphoma n = 1, gliosis n = 1).

In six clinical groups, mean CBI ± s.e. (standard error) was calculated (astrocytoma I–II n =8, mean CBI = 0.732 ± 0.058; astrocytoma III n = 10, mean CBI = 0.762 ± 0.098; glioblastoma IV n = 12, mean CBI = 0.816 ± 0.12; meningioma n = 19, mean CBI = 1.075 ± 0.087; angioma n = 3, mean CBI = 0.906 ± 0.171; metastases n = 10, mean CBI = 0.693 ± 0.081). Mean CBI slightly increased with malignancy of gliomas (ANOVA within histologic subclassification revealed no significance). In meningiomas, generally the highest tracer deposit was observed. Statistical comparison (ANOVA) of CBIs revealed significant differences between meningiomas and each of the three glioma subgroups (DF = 3; F = 2.914; $p < 0.05$) (Fig. 5).

Correlation of HMPAO Uptake and GSH Content

In cases where biopsy specimens were obtained during surgery, ROIs were drawn corresponding to the location of tissue probes (see Materials and Methods). A cerebellar index [CBI = average cts per pixel (specimen ROI)/average cts per pixel (cerebellar ROI)] was calculated and correlated with GSH values by linear regression analysis. The

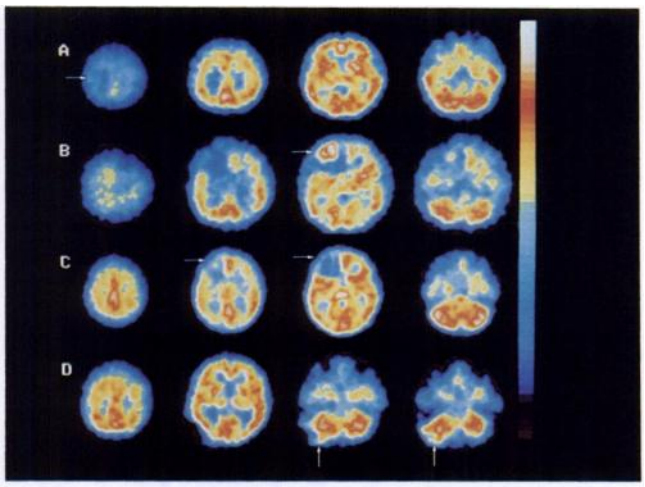

FIGURE 4. Metastases. (A) Transverse cross sections in a 51-yr-old female with a cerebral metastasis originating from a peripheral bronchial neoplasm. SPECT shows low uptake in the left parietal region. CBI = 0.5. (B) Transverse cross sections in a 63-yr-old male suffering from hypernephroma. SPECT shows high uptake in the left superior frontal region surrounded from a low uptake zone (edema). CBI = 1.09, GSH = 1.37 nmol/mg. (C) Transverse cross sections in a 37-yr-old female with melanoma. Uptake deficiency in the left frontal lobe is revealed by SPECT. No CCD can be observed. CBI = 0.51. (D) Transverse cross sections in a 77-yr-old male with cerebellar symptoms. SPECT shows abnormally configurated uptake in the left cerebellum, indicating a metastasis of an anaplasic epithelial tumor of unknown origin. The highly malignant neoplasm infiltrated locally into the skull. CBI = 0.986, GSH = 0.907 nmol/mg.

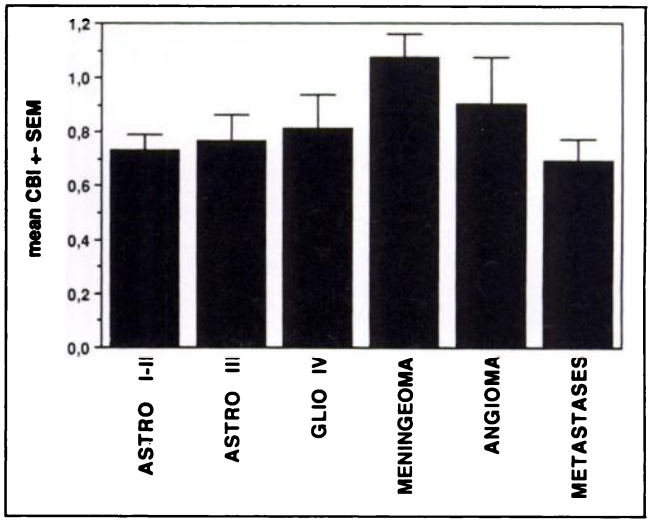

FIGURE 5. Mean cerebellar index (CBI) ± s.e. in astrocytoma I–II (n = 8), astrocytoma III (n = 10), glioblastoma IV (n = 12), meningioma (n = 19), angioma (n = 3), and in an inhomogenous group containing metastases (n = 10) ANOVA revealed significant ($p < 0.05$) differences between CBIs in meningiomas compared with astrocytoma I–II, astrocytoma III and glioblastoma IV, respectively.

results are shown for all samples (n = 32; y = 4.899x − 1.527; r = 0.80; p < 0.001) (Fig. 6). When calculating data from meningiomas (n = 10; y = 4.0498x − 0.394; r = 0.863; p < 0.01) and gliomas (n = 15; y = 5.0385x − 1.926; r = 0.68; p < 0.01) separately, linear regression analysis yields a significant correlation between GSH and CBI values in each group respectively. In contrast, no correlation was found in metastases (n = 5; y = 5.11x − 1.38; r = 0.36; n.s.). It is remarkable that even when GSH was not detectable, HMPAO uptake was observed in all groups. This indicates that factors in addition to GSH might contribute to HMPAO conversion in vivo.

GSH levels in normal brain tissues reportedly vary between 1–10 m*M* (*10*). For tumor tissues, data about increased GSH levels are established. In this study, higher GSH values (mean ± s.e.) were found in meningiomas (n = 8, mean GSH = 3.861 ± 0.793 nmol/mg) and in normal cortex (n = 3, mean GSH = 2.72 ± 0.55 nmol/mg) than in gliomas (n = 14, mean GSH = 1.547 ± 0.306 nmol/mg). Independent t-test revealed significant differences of GSH values between meningiomas and gliomas (n = 22; t = 3.229; p < 0.004; data not shown). Due to the small number of samples, data from normal cortex (two patients with meningiomas and one with glioma) were not taken into consideration for statistics.

Estimation of Tumor Vascularization

In normal brain tissue, about 0.3% of the injected activity was assumed to represent the vascular compartment, resulting in a CBF:CBV ratio of about 17:1 (*7*). For estimation of the vascular compartment in tumors, Mab Factor VIII immunostaining of tissue probes (see Materials and Methods) was performed. No significant correlation between CBIs and values representing vascular density was found (n = 11; y = 0.398 ± 0.169x; r = 0.589; n.s. data not shown). It was therefore assumed, that the contribution of tumor blood volume to the registered counts in tumor ROIs is negligible. This result agrees well with the observation that dynamic SPECT scanning during the initial passes of HMPAO shows high tracer concentrations in highly vascularized tumors (i.e., angiomas) followed by a rapid washout. Only in one angioma, high tracer uptake was seen (Fig. 3). This controversial observation may be due to tracer deposit in endothelium. Likewise, in meningiomas containing high amounts of endothelial structures, a trend towards higher uptake than in predominantly fibroblastic lesions was observed (independent t-test: n = 19; t = 2.252; p < 0.038; data not shown).

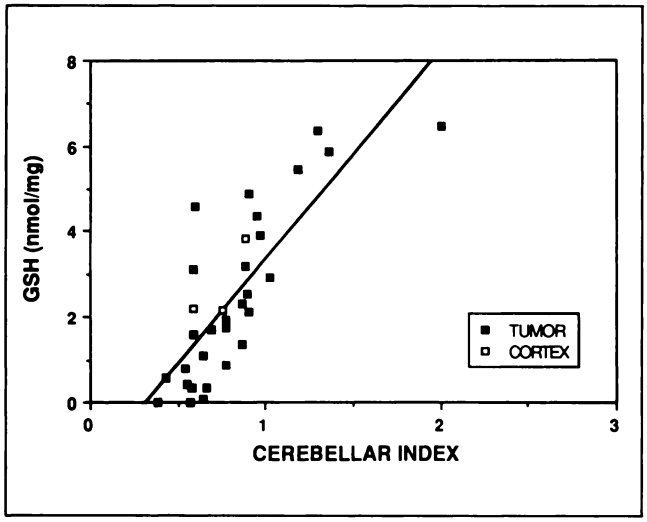

FIGURE 6. Correlation of CBIs and GSH concentration in all samples (glioma n = 15; meningioma n = 10; metastasis n = 5; neurocytoma n = 1; neuroma n = 1) (n = 32; y = −1.527 + 4.899x; r = 0.80; p < 0.001). The data set contains three samples from nonaffected cortical tissue (CORTEX) in tumor patients.

DISCUSSION

Several factors account for the problems in quantification of HMPAO SPECT data. First, the lipophilic complex degrades spontaneously to hydrophilic products. This process is dependent on the time since eluation of technetium, the tracer concentration added to the uncomplexed ligand, pH and the presence of reducing agents (*17*). In the blood, HMPAO is retained by leukocytes and reversibly bound to proteins. In addition, a dependency of this process on bolus size was proposed. Thus, the estimation of the extractable fraction from blood remains problematic. Within the brain, HMPAO follows CBF at normal flow, while low flow is slightly overestimated and high flow is underestimated (*18*). In high flow areas, it was assumed that flow competes with the intracellular conversion rate of the ligand. Although the non-linearity of HMPAO distribution in relation to flow was proposed to be correctable (*19*), the obtained gray/white matter contrast-enhancement in tumor patients was still significantly below PET values (*9*). HMPAO freely passes the intact blood-brain barrier, but in the cell the conversion to hydophilic derivates was proposed to be dependent on GSH (*10*). While the extraction efficiencies of both meso- and d,l-HMPAO were assumed to be identical, the conversion rate of meso-HMPAO was found to be an order of magnitude below the one of the d,l-mixture in vitro. That observation lead to the conclusion that meso-HMPAO reflects a map of the conversion rate or organ GSH concentration rather than blood flow. This hypothesis, however, could not be confirmed in a study investigating the relationship between GSH concentration and the retention of meso-HMPAO in lung tumors (*20*). Since the most critical assumption of the model is a uniform conversion rate in different kinds of tissues, variations of this rate may account for the discrepancy. In our study, no significant correlation between d,l-HMPAO uptake and GSH content in metastases of non-cerebral origin was found. If a fixed relation between regional blood flow and the local conversion rate of the lipophilic complex determined the distribution of HMPAO, the lung uptake of HMPAO should be very high since lung blood flow is

higher than CBF (*21*). The significant correlation between regional tracer retention and GSH content in brain tumors as described in this study does not necessarily contradict the hypothesis mentioned above. Data from in vitro studies on the retention of d,l-HMPAO in cultured neurons of the rat cerebellum confirm the observation made in brain tumors and SPECT (*22*). Both studies, however, show that additional factors yet unknown contribute to the (low) tracer retention in the absence of GSH. Fractions of intracellular d,l-HMPAO reportedly bound to proteins in the cytosol may account for this observation (*23*).

For reasons discussed above, quantification of rCBF using d,l-HMPAO SPECT is not yet possible in a generally accepted manner. Instead, we decided to calculate a tumor-to-cerebellum ratio for semiquantitative evaluation of tracer retention. The ipsilateral cerebellum was chosen as a reference to avoid errors, caused by CCD as observed in 21 cases. Interhemispheric comparison was not performed since many tumors (especially Grade IV gliomas) had crossed the midline or were placed in the midline (meningiomas), while others (neuroma) had no contralateral anatomical counterpart.

For statistical analysis, data were classified according to tumor classification verified by histologic diagnosis. In gliomas, some tissue probes were composed of multiple stages of differentiation. Therefore low-grade astrocytomas (I–II) were pooled in one group. In Grade II–III and Grade III–IV gliomas, the higher malignancy was taken as classification criterion in case of uncertainty. Grade IV glioblastomas were very often composed of both, high and low uptake zones in SPECT images, due to central necrosis and perifocal edema. This phenomenon, as well as overlapping stages of tissue differentiation, may have masked the significance of statistical comparison within gliomas. Highest tracer deposit was found in meningiomas (except in calcified ones) and in some metastases. This observation agrees well with quantitative tumor blood flow data obtained by N-iso-propyl-p-iodo-amphetamine (^{123}I) SPECT in meningiomas (*24,25*).

The distribution of d,l-HMPAO seen in SPECT images is closely related to tumor blood flow (*9*). The results obtained in our study are in good agreement with previous reports on this issue (*7,9*). Since the HMPAO distribution most likely is dependent on both CBF and GSH concentration, one may conclude, that HMPAO SPECT images reveal information about both variables.

Statistical comparison of CBIs and GSH content in tumor specimens yielded a significant correlation. Since ROIs were drawn in approximate correspondance to the locations the specimens were taken from, and clearly exceeded the size of tissue probes to avoid errors due to the partial volume effect, one would expect a loss of significance for methodologic reasons. Although our result suggests the contribution of additional factors, it strongly supports the hypothesis, that GSH is the predominant mediator of d,l-HMPAO conversion to hydrophilic derivates.

CONCLUSION

The aim of this study was to prove the assumption that GSH is the rate determining compound for the conversion of the lipophilic complex and to evaluate the use of (^{99m}Tc)-d,l-HMPAO SPECT in the diagnosis of brain tumors.

Our results are in good agreement with previous reports on d,l-HMPAO retention in brain tumors. They confirm our experience with the visual evaluation of SPECT images in that uptake behavior provides complementary information for the diagnosis and estimation of malignancy in brain tumors. Additional factors, however, such as typical location, extention and inhomogeneity of tracer deposit within tumor borders, as well as perifocal edema must be considered. Individual exceptions of typical uptake behavior, as shown in meningiomas and angiomas, as well as the variability of tracer deposit common to high-grade gliomas and metastases, indicate the d,l-HMPAO retention in brain tumors is nonspecific.

The correlation between CBI and GSH varies across different tumor groups. Gliomas and meningiomas show a highly significant correlation, whereas metastases do not. This discrepancy may either be due to tissue specific factors, such as a different conversion rate of d,l-HMPAO or the inhomogeneous and relatively small case load. Recent studies suggest that high GSH levels may be related to tumor cell resistance in cytoreductive chemotherapy (i.e., BCNU). Tumor imaging with d,l-HMPAO may be able to offer prognostic information about the efficacy of therapy that interferes with this system (*26,27*).

REFERENCES

1. Nowotnik DP, Canning LR, Cummings SA, et al. Development of a ^{99m}Tc radiopharmaceutical for cerebral blood flow imaging. *Nucl Med Commun* 1985;6:499–506.
2. Sharp PF, Smith FW, Gemmel HG, et al. Technetium-99m-HM-PAO stereoisomers as potential agents for imaging regional cerebral blood flow: human volunteer studies. *J Nucl Med* 1986;27:171–177.
3. Ell PJ, Hocknell JMI, Jarritt PH, et al. A ^{99m}Tc-labelled radiotracer for the investigation of cerebral vascular disease. *Nucl Med Commun* 1985;6:437–441.
4. Podreka I, Suess E, Goldenberg G, et al. Initial experience with technetium-99m-HM-PAO Brain Spect. *J Nucl Med* 1987;28:1657–1666.
5. Hammersley PAG, McCready R, Babich JW, et al. ^{99m}Tc-HMPAO as a tumor blood flow agent. *Eur J Nucl Med* 1987;13:90–94.
6. McCready VR, Babich J, Flower MA, et al. The use of ^{99m}Tc-HMPAO for the study of tumor blood flow. *Nucl Med* 1988;27:116–117.
7. Lindegaard MW, Skretting A, Hager B, et al. Cerebral and cerebellar uptake of ^{99m}Tc-(d,l)-hexamethyl-propyleneamine oxime (HM-PAO) in patients with brain tumor studied by single photon emission computerized tomography. *Eur J Nucl Med* 1986;12:417–420.
8. Babich JW, Keeling F, Flower MA, et al. Initial experience with Tc-99m-HM-PAO in the study of brain tumors. *Eur J Nucl Med* 1988;14:39–44.
9. Langen KJ, Herzog H, Kuwert T, et al. Tomographic studies of rCBF with (^{99m}Tc)-HM-PAO SPECT in patients with brain tumors: comparison with C1502 continuous inhalation technique and PET. *J Cereb Blood Flow Metab* 1988;8:90–94.
10. Neirinckx RD, Burke JF, Harrison RC, et al. The retention mechanism of technetium-99m-HM-PAO: intracellular reaction with glutathione. *J Cereb Blood Flow Metab* 1988;8(suppl 1):S4–S12.
11. Orlowski M, Karkowsky A. Glutathione metabolism and some possible functions of glutathione in the nervous system. *Int Rev Neurobiol* 1976;19:75–121.
12. Podreka I, Baumgartner C, Suess E, et al. Quantification of regional cerebral blood flow with IMP-SPECT. *Stroke* 1988;20:183–191.

13. Mazziotta JC, Phelps ME, Plummer D, et al. Quantification in positron emission computed tomography. 5. Physical-anatomical effects. *J Comput Assist Tomogr* 1981;5:734–743.
14. Langen KJ, Roosen N, Herzog H, et al. Investigation of brain tumors with ^{99m}Tc-HMPAO SPECT. *Nucl Med Commun* 1989;10:325–334.
15. Lee FYF, Allalunis-Turner MJ, Siemann DW. Depletion of tumor versus normal tissue glutathione by buthionine sulfoximine. *Br J Cancer* 1987;56:33–38.
16. Weibel ER. Practical methods for biological morphometry. In: *Stereological Methods, volume 1.* London, New York: Academic Press; 1979.
17. Hung JC, Corlija M, Volkert A, et al. Kinetic analysis of technetium-99m-d,l-HM-PAO decomposition in aqueous media. *J Nucl Med* 1988;29:1568–1576.
18. Hoffman TJ, Corlija M, Chaplin SB, et al. Retention of (^{99m}Tc)-d,l-HM-PAO in rat brain: an autoradiographic study. *J Cereb Blood Flow Metab* 1988;8:38–43.
19. Lassen NA, Andersen AR, Friberg L, et al. The retention of (99mTc)-d,l-HMPAO in the human brain after intracarotid bolus injection: a kinetic analysis. *J Cereb Blood Flow Metab* 1988;8(suppl 1):S12–S22.
20. Rowell NP, McCready VR, Cronin B, et al. ^{99m}Tc-labelled meso-HMPAO and glutathione content of human lung tumors. *Nucl Med Commun* 1989;10:503–508.
21. Costa DC, Ell PJ, Cullum ID, et al. The in vivo distribution of ^{99m}Tc-HM-PAO in normal man. *Nucl Med Commun* 1986;7:647–658.
22. Suess E, Huck S. (^{99m}Tc)-d,l-HMPAO accumulation in cultured neurons. *J Cereb Blood Flow Metab* 1989;9(suppl 1):S735.
23. Costa DC, Lui D, Sinha AK, et al. Intracellular localisation of ^{99m}Tc-d,l-HMPAO and ^{201}Tl-DDC in rat brain. *Nucl Med Commun* 1989;10:459–466.
24. Nakano S, Kinoshita K, Jinnouchi S, et al. Dynamc SPECT with iodine-123-IMP in meningiomas. *J Nucl Med* 1988;29:1627–1632.
25. Nishimura T, Hayashida K, Uehara T, et al. Two patients with meningioma visualized as high uptake by SPECT with N-isopropyl-p-iodo-amphetamine (I-123). *Neuroradiology* 1988;30:351–354.
26. Ali-Osman F, Caughlan J, Gray DS. Decreased DNA interstrand cross-linking and cytotoxicity induced in human brain tumors by 1,3-bis-(2-chloroethyl)-1-nitrosurea after in vitro reaction with glutathione. *Cancer Res* 1989;49:5954–5958.
27. Evans CG, Bodell WJ, Ross D, et al. Role of glutathione and related enzymes in brain tumor cell resistance to BCNU and nitrogen mustard [Abstract]. *Proc Ann Meet Am Soc Cancer Res* 1986;27:267.

EDITORIAL

Technetium-99m-HMPAO Retention and the Role of Glutathione: The Debate Continues

Many patients presenting with primary brain tumors face a grim prognosis due to the inability to control local disease (*1*). Secondary brain tumors present similar therapeutic difficulties, although survival probably depends more on the extent of extra-cerebral disease (*2*). However, as more aggressive antineoplastic regimens begin to demonstrate greater control of systemic disease, survival may depend on adequate treatment of central nervous system secondaries.

Tumor perfusion may play an important role in the success of antineoplastic therapies such as radiotherapy and chemotherapy due to their dependence on adequate blood flow for oxygenation and drug transport, respectively. A noninvasive means of studying brain tumor blood flow should help us to improve our understanding of the role perfusion plays in brain tumor therapy and prognosis.

rCBF TRACERS

Regional cerebral blood flow (rCBF) tracers for use with single-photon emission tomography (SPECT) must possess, amongst other characteristics, a mechanism by which the activity extracted into the brain is fixed for a sufficient time to allow for image acquisition. In order to accomplish this, a "trapping" mechanism must exist. Ideally, a prerequisite for the trapping mechanism is that it is unaffected by pathology. It is then possible to begin to interpret tracer distribution images as true rCBF images in a range of disorders.

The ability to image regional rCBF using nondynamic SPECT was brought about by the introduction of the ^{123}I-labeled-amines; IMP (p-iodo-N-isopropyl amphetamine) (*3*) and HIPDM (N,N,N,-trimethyl-N-[2-hydroxy-3-methyl-5-iodobenzyl]-1,3-propanediamine) (*4*). Both compounds demonstrated high first-pass extraction in the brain and prolonged retention. While the exact "trapping" mechanism of the amines remains uncertain (*5*), they have proved useful in aiding the diagnosis of both cerebrovascular and neurologic disorders (*6–8*).

The application of these early SPECT tracers excluded the study of neurooncology due to the reported lack of a functional trapping mechanism in primary brain tumors (*9–11*), although there were reports of uptake in metastases to brain (*12,13*) and in isolated cases of primary brain tumors (*14*).

Technetium-99m-HMPAO

Technetium-99m-d,l-HMPAO (exametazime) is the first clinically available ^{99m}Tc-labeled rCBF tracer. This tracer exhibits high first-pass extraction in the brain and prolonged retention, making it suitable for SPECT imaging using non-dynamic systems (*15,16*). Initial studies in patients with brain tumors indicated that, unlike IMP and HIPDM, this new tracer was capable of localizing in primary brain tumors (*17*).

The cerebral retention of ^{99m}Tc-HMPAO is believed to involve the intracellular conversion of the hydrophobic Tc-HMPAO to a species which is incapable of rapid back diffusion. The proposed mechanism of this conversion is thought to involve interaction of ^{99m}Tc-HMPAO with glutathione (GSH) (18). This theory is based on the similarity in measured conversion rates of ^{99m}Tc-d,l-HMPAO (to a less hydrophobic species) when ex-

Received Apr. 4, 1991; revision accepted Apr. 23, 1991.
For reprints contact: J.W. Babich, Massachusetts General Hospital-East, Room 5406, Bldg. 149, 13th St., Charlestown, MA 02129.